version 16 August 24, 2000

Elliptic flow in Au+Au collisions at $\sqrt{s_{NN}} = 130$ GeV

K.H. Ackermann[19], N. Adams[28], C. Adler[12], S. Ahmad[28], Z. Ahammed[27], C. Allgower[13], J. Amsbaugh[34], E. Anderssen[17], M. Anderson[6], H. Arnesen[3], L. Arnold[14], G.S. Averichev[10], S. Bekele[24], A. Baldwin[16], J. Balewski[13], L.S. Barnby[16], O. Barannikova[10,27], J. Baudot[14], M. Beddo[1], V.V. Belaga[10], R. Bellwied[35], S. Bennett[35], J. Bercovitz[17], J. Berger[12], W. Betts[24], H. Bichsel[34], F. Bieser[17], L.C. Bland[13], M. Bloomer[17], C.O. Blyth[4], J. Boehm[17], A. Bogdanov[21], B.E. Bonner[28], D. Bonnet[14], R. Bossingham[17], M. Botlo[3], A. Boucham[30], N. Bouillo[30], S. Bouvier[30], K. Bradley[17], F.P. Brady[6], E.S. Braithwaite[2], W. Braithwaite[2], R. L. Brown[3], G. Brugalette[34], C. Byrd[2], H. Caines[24], M. Calderón de la Barca Sánchez[36], A. Cardenas[27], L. Carr[34], J. Carroll[17], J. Castillo[30], B. Caylor[17], D. Cebra[6], S. Chatopadhyay[35], M.L. Chen[3], W. Chen[3], Y. Chen[7], S.P. Chernenko[10], M. Cherney[9], A. Chikanian[36], B. Choi[31], J. Chrin[9], W. Christie[3], J.P. Coffin[14], L. Conin[30], C. Consiglio[3], T.M. Cormier[35], J.G. Cramer[34], H.J. Crawford[5], V.I. Danilov[10], D. Dayton[3], M. DeMello[28], A.A. Derevschikov[26], W.S. Deng[16], M. Dialinas[30], H. Diaz[3], P.A. DeYoung[8], L. Didenko[3], D. Dimassimo[3], J. Dioguardi[3], W. Dominik[32], C. Drancourt[30], J.E. Draper[6], V.B. Dunin[10], J.C. Dunlop[36], W.R. Edwards[17], V. Eckardt[19], L.G. Efimov[10], T. Eggert[19], V. Emelianov[21], J. Engelage[5], G. Eppley[28], B. Erazmus[30], A. Etkin[3], P. Fachini[29], V. Faine[3], C. Feliciano[3], D. Ferenc[6], M.I. Ferguson[7], H. Fessler[19], E. Finch[36], Y. Fisyak[3], D. Flierl[12], I. Flores[5], K.J. Foley[3], D. Fritz[17], N. Gagunashvili[10], J. Gans[36], M. Gazdzicki[12], M. Germain[14], F. Geurts[28], V. Ghazikhanian[7], C. Gojak[14], J. Grabski[33], O. Grachov[35], M. Grau[3], D. Greiner[17], L. Greiner[5], V. Grigoriev[21], D. Grosnick[1], J. Gross[9] G. Guilloux[30], E. Gushin[21], J. Hall[35], T.J. Hallman[3], D. Hardtke[17], G. Harper[34], J.W. Harris[36], P. He[5], M. Heffner[6], S. Heppelmann[25], T. Herston[27], D. Hill[1], B. Hippolyte[14], A. Hirsch[27], E. Hjort[27], G.W. Hoffmann[31], M. Horsley[36], M. Howe[34], H.Z. Huang[7], T.J. Humanic[24], H. Hümmler[19], W. Hunt[13], J. Hunter[17], G.J. Igo[7], A. Ishihara[31], Yu.I. Ivanshin[11], P. Jacobs[17], W.W. Jacobs[13], S. Jacobson[17], R. Jared[17], P. Jensen[31], I. Johnson[17], P.G. Jones[4], E. Judd[5], M. Kaplan[8], M. Kaneta[17], A. Karakash[21], D. Keane[16], V.P. Kenney[23,*], J. Klay[6], S.R. Klein[17], A. Klyachko[13], G. Koehler[17], A.S. Konstantinov[26], V. Kormilitsyne[7,26], L. Kotchenda[21], I. Kotov[24], A.D. Kovalenko[10], M. Kramer[22], P. Kravtsov[21], K. Krueger[1], T. Krupien[3], P. Kuczewski[3], C. Kuhn[14], G.J. Kunde[36], C.L. Kunz[8], R.Kh. Kutuev[11], A.A. Kuznetsov[10], L. Lakehal-Ayat[30], M.A.C. Lamont[4], J.M. Landgraf[3], S. Lange[12], C.P. Lansdell[31], B. Lasiuk[36], F. Laue[24], A. Lebedev[3], W.J. Leonhardt[3], V.M. Leontiev[26], P. Leszczynski[33], T. LeCompte[1], M.J. LeVine[3], Q. Li[35], Q. Li[17], Z. Li[3], C.-J. Liaw[3], J. Lin[9], S.J. Lindenbaum[22], V. Lindenstruth[5], P.J. Lindstrom[5], H. Liu[16], M.A. Lisa[24], T. Ljubicic[3], W.J. Llope[28], G. LoCurto[19], H. Long[7], R.S. Longacre[3], M. Lopez-Noriega[24], D. Lopiano[1], W.A. Love[3], J.R. Lutz[14], D. Lynn[3], L. Madansky[15,*], R. Majka[36], A. Maliszewski[33], S. Margetis[16], R. Maier[19], L. Martin[30], K. Marks[17], R. Marstaller[19], J. Marx[17], H.S. Matis[17], Yu.A. Matulenko[26], E.A. Matyushevski[10], C. McParland[17], T.S. McShane[9], J. Meier[9], N. Mikhalin[7,26], Yu. Melnick[26], A. Meschanin[26], P. Middlekamp[3], B. Miller[3], Z. Milosevich[8], N.G. Minaev[26], B. Minor[17], J. Mitchell[15], E. Mogavero[3], V.A. Moiseenko[11], D. Moltz[17], V. Morozov[17], R. Morse[17], C.F. Moore[31], M.M. de Moura[29], M.G. Munhoz[29], G.S. Mutchler[28], J.M. Nelson[4], P. Nevski[3], T. Ngo[7], M. Nguyen[3], T. Nguyen[3], V.A. Nikitin[11], L.V. Nogach[26], T. Noggle[17], B. Norman[16], S.B. Nurushev[26], T. Nussbaum[28], J. Nystrand[17], G. Odyniec[17], A. Ogawa[25], C. Ogilivie[18], V. Okorokov[21], K. Olchanski[3], M. Oldenburg[19], D. Olson[17], G.A. Ososkov[10], G. Ott[31], D. Padrazo[3], G. Paic[24], S.U. Pandey[35], Y. Panebratsev[10], S.Y. Panitkin[16], A.I. Pavlinov[26], T. Pawlak[33], M. Pentia[10], W. Peryt[33], V. Perevotchikov[3], V.A Petrov[11], W. Pinganaud[30], S. Pirogov[7], E. Platner[28], J. Pluta[33], I. Polk[3], N. Porile[27], J. Porter[3], A.M. Poskanzer[17], D. Prindle[34], E. Potrebenikova[10], C. Pruneau[35], J. Puskar-Pasewicz[13], G. Rai[17], J. Rasson[17], O. Ravel[30], R.L. Ray[31], S.V. Razin[10,13], D. Reichhold[9], J. Reid[34], R.E. Renfordt[12], F. Retiere[30], A. Ridiger[21], J. Riso[35], HG. Ritter[17], J.B. Roberts[28], D. Roehrich[12], O.V. Rogachevski[10], J.L. Romero[6], C. Roy[30], M. Runco[21], D. Russ[8], V. Rykov[35], I. Sakrejda[17], R. Sanchez[7], Z. Sandler[7], J. Sandweiss[36], P. Sappenfield[28], A.C. Saulys[3], I. Savin[11], J. Schambach[31], R.P. Scharenberg[27], J. Scheblien[3], R. Scheetz[3], R. Schlueter[17], A. Schüttauf[19], N. Schmitz[19], L.S. Schroeder[17], M. Schulz[3,19], J. Sedlmeir[3], J. Seger[9], D. Seliverstov[21], J. Seyboth[19], P. Seyboth[19], R. Seymour[34], E.I. Shakaliev[10], A. Shalnov[21], K.E. Shestermanov[26], Y. Shi[7], S.S. Shimanskii[10], D. Shuman[17], V.S. Shvetcov[11], G. Skoro[10], N. Smirnov[36], L.P. Smykov[10], R. Snellings[17], K. Solberg[13], J. Sowinski[13], H.M. Spinka[1], B. Srivastava[27], E.J. Stephenson[13], R. Stock[12], A. Stolpovsky[35], N. Stone[3], R. Stone[17], M. Strikhanov[21], B. Stringfellow[27], H. Stroebele[12], C. Struck[12], A.A.P. Suaide[29], E. Sugarbaker[24], C. Suire[14], T.J.M. Symons[17], J. Takahashi[29], A.H. Tang[16], A. Tarchini[14], J. Tarzian[17], A. Szanto de Toledo[29], J.H. Thomas[17], V. Tikhomirov[21], S. Tonse[17], T. Trainor[34], S. Trentalange[7], M. Tokarev[10], M.B. Tonjes[20], V. Trofimov[21], O. Tsai[7], K. Turner[3], T. Ullrich[36], D.G. Underwood[1], I. Vakula[7], G. Van Buren[3], A.M. VanderMolen[20], A. Vanyashin[17], A.N. Vasiliev[26], I.M. Vasilevski[11], S.E. Vigdor[13], G. Visser[5], S.A. Voloshin[35], C. Vu[17], F. Wang[27], H. Ward[31], D. Weerasundara[34], R. Weidenbach[17], R. Wells[17], R. Wells[24], T. Wenaus[3], G.D. Westfall[20], J.P. Whitfield[8], C. Whitten Jr. [7], H. Wieman[17], R. Willson[24], K.Wilson[35], J. Wirth[17], J. Wisdom[7], S.W. Wissink[13], R. Witt[16], J. Wolf[17], L. Wood[6], N. Xu[17], Z. Xu[36], E. Yamamoto[7], J. Yang[7], A.E. Yakutin[26], P. Yepes[28], A. Yokosawa[1], V.I. Yurevich[10], Y.V. Zanevski[10], J. Zhang[17], W.M. Zhang[16], J. Zhu[34], D. Zimmerman[17], R. Zoulkarneev[11], A.N. Zubarev[10]

(STAR Collaboration)

[1] *Argonne National Laboratory,* [2] *University of Arkansas, Little Rock,* [3] *Brookhaven National Laboratory,* [4] *University of Birmingham,* [5] *University of California, Berkeley,* [6] *University of California, Davis,* [7] *University of California, Los Angeles,* [8] *Carnegie Mellon University,* [9] *Creighton University,* [10] *Laboratory for High Energy (JINR), Dubna,* [11] *Particle Physics Laboratory (JINR), Dubna,* [12] *University of Frankfurt,* [13] *Indiana University,* [14] *Institut de Recherches Subatomiques,* [15] *The Johns Hopkins University,* [16] *Kent State University,* [17] *Lawrence Berkeley National Laboratory,* [18] *Massachusetts Institute of Technology,* [19] *Max-Planck-Institut fuer Physik, Munich,* [20] *Michigan State University,* [21] *Moscow Engineering Physics Institute,* [22] *City College of New York,* [23] *University of Notre Dame,* [24] *Ohio State University,* [25] *Pennsylvania State University,* [26] *Institute of High Energy Physics, Protvino,* [27] *Purdue University,* [28] *Rice University,* [29] *Universidade de Sao Paulo,* [30] *SUBATECH, Nantes,* [31] *University of Texas, Austin,* [32] *Warsaw University,* [33] *Warsaw University of Technology,* [34] *University of Washington,* [35] *Wayne State University,* [36] *Yale University*

(August 24, 2000)

Elliptic flow is one of the hadronic observables sensitive to the very early stages of the evolution of the system created in nuclear collisions. We report first results on elliptic flow of charged particles at midrapidity in Au+Au collisions at $\sqrt{s_{NN}} = 130$ GeV using the STAR TPC at RHIC. The elliptic flow signal, v_2, averaged over transverse momentum, reaches values of about 6% for relatively peripheral collisions and decreases for the most central collisions. Pseudorapidity and transverse momentum dependence of elliptic flow are also presented.

The goal of the ultrarelativistic nuclear collision program is the creation of a system of deconfined quarks and gluons [1]. If this system is created, its evolution should be governed by the physics of deconfined matter. Elliptic flow, one of the observables sensitive to the early evolution of the system, is the anisotropic emission of particles "in" or "out" of the reaction plane defined for non-central collisions by the beam direction (z-axis) and the impact parameter direction (x-axis). Elliptic flow is usually characterized in terms of particle momenta by $v_2 = \langle (p_x^2 - p_y^2)/(p_x^2 + p_y^2) \rangle$, the second harmonic Fourier coefficient in the azimuthal distribution of particles with respect to the reaction plane [2,3]. Originally, the system is not azimuthally symmetric due to the non-centrality of the collision. Elliptic flow has its origin in this spatial anisotropy of the system when it is created, and in particle rescatterings in the evolving system which convert the spatial anisotropy to momentum anisotropy. The spatial anisotropy in general decreases with system expansion, thus quenching this driving force and making elliptic flow particularly sensitive to the early stages of the system evolution [4]. Being dependent on rescattering, elliptic flow is sensitive to the degree of thermalization of the system [5,6] at this early time. Theoretically, hydrodynamic models which are based on the assumption of complete local thermalization, could be expected to predict the strongest signals, and they do [6–9].

Elliptic flow in ultrarelativistic nuclear collisions was first discussed in Ref. [7] and has been studied intensively in recent years at AGS [10,11] and SPS [12–14] energies. These studies found that elliptic flow at high energies is "in-plane", $v_2 > 0$, as expected from most models, and the pion elliptic flow for relatively peripheral collisions increases with beam energy [15] from about 2% at the top AGS energy [10] to about 3.5% at the SPS [13]. The experimental results can be interpreted as an approach to early thermalization as the beam energy increases [5]. From transport cascade models for the full RHIC energy, a peak elliptic flow value of 1.5% is predicted by UrQMD [16] calculations and 2.5% by RQMD v2.4 [17] calculations [18]. Hydrodynamic models predict v_2 as high as 10% [6,8]. Most importantly, the details of the v_2 dependence on beam energy as well as its dependence on centrality are thought to be sensitive to the phase transition between confined and deconfined matter [5,6,8,9,19] (see also [15] and references therein).

We report here the first results on elliptic flow in Au+Au collisions at the Relativistic Heavy Ion Collider (RHIC) at $\sqrt{s_{NN}} = 130$ GeV. The Solenoidal Tracker At RHIC (STAR) [20] consists of several detector subsystems in a large solenoidal magnet. For first year data taking, the setup consists of the Time Projection Chamber (TPC) which covers the pseudorapidity range $|\eta| < 1.8$ for collisions in the center of the TPC, and has complete azimuthal coverage, which is desirable for the study of azimuthal correlations. In the first year, the TPC is operated with a 0.25 Tesla field, allowing tracking of particles with $p_t > 75$ MeV/c. Two Zero Degree Calorimeters [21] which measure fragmentation neutrons were used in coincidence for the trigger. The TPC is surrounded by a scintillator barrel which measures the charged particle multiplicity, and is used in studies of the trigger performance and vertex reconstruction efficiency.

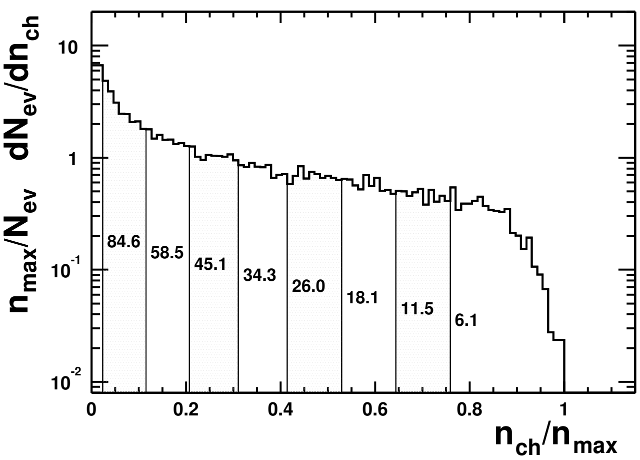

FIG. 1. The primary track multiplicity distribution as a function of the number of tracks normalized by the maximum observed number of tracks. The eight centrality regions used in this analysis are shown. The integral under the curve is 1.0 and the cumulative fraction corresponding to the lower edge of each centrality bin is also indicated in percent.

The relative multiplicity distribution for events with a reconstructed primary vertex is shown in Fig. 1. An analysis of the trigger performance and vertex reconstruction efficiency, together with comparisons with Hijing [22], show that the events in Fig. 1 are hadronic Au+Au interactions corresponding to about 90% of the geometric cross section, the remaining being attributed to vertex reconstruction inefficiency for low-multiplicity events. This vertex finding inefficiency is not included in the normalization of Fig. 1. The multiplicity is the number of primary tracks which pass within 3 cm of the vertex and have $|\eta| < 0.75$. The distribution shown is not corrected for tracking efficiency, since it is used in this analysis only for centrality determination.

For this analysis, 22 k events were selected with a primary vertex position within 75 cm longitudinally of the TPC center and within 1 cm radially of the beam line. Tracks were selected with $0.1 < p_t \leq 2.0$ GeV/c in order to have an efficiency constant to within ± 10%. They also passed within 1 cm of the primary vertex, had at least 15 hits, and $|\eta| < 1.3$. For the determination of the event plane we required $|\eta| < 1.0$. Also, the ratio of hits to the expected maximum number of hits for that particular track was required to be greater than 0.52, largely suppressing split tracks from being counted twice. However, the analysis results were not sensitive to these cuts.

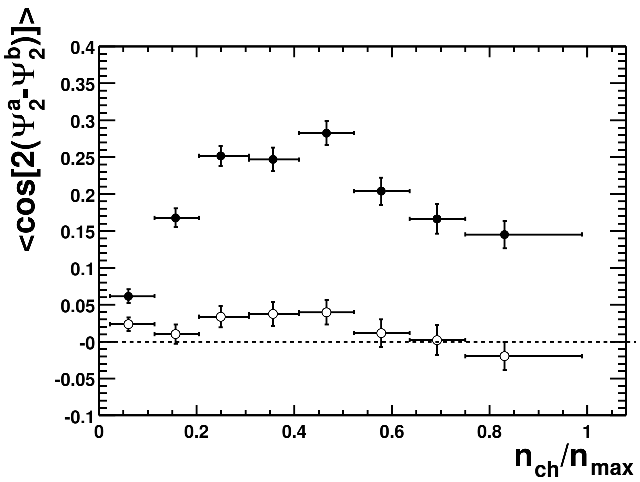

FIG. 2. Correlation between the event plane angles determined for two independent subevents. The upper set of data is for the second harmonic and the lower set is $\langle\cos(\Psi^a - \Psi^b)\rangle$ for the first harmonic. The points are positioned at the values of mean n_{ch}/n_{max} corresponding to each of the centrality bins in Fig.1. The horizontal bars show the widths of the bins.

The analysis method [2,3] involves calculation of the second harmonic event plane angles, Ψ_2, for two subevents, which are groups of independent particles from the same event. In order to see whether these planes are correlated, the mean cosine of the difference in their event plane angles is calculated. The subevents have been chosen in three different ways: 1) Assigning particles with pseudorapidity $0.05 < \eta < 1$ to one subevent and particles with $-1 < \eta < -0.05$ to the other subevent. The "gap" between the two regions ensures that short range correlations, such as Bose-Einstein correlations or Coulomb final state interactions, contribute negligibly to the observed correlation. 2) Dividing all particles randomly into two subevents. 3) Assigning positive particles to one subevent and negative particles to the other. Fig. 2 shows the results for correlation of the event planes of subevents assigned by the pseudorapidity method. The random method and the charge method give similar results. Non-flow effects (not correlated with the reaction plane) would contribute differently for these different subevent choices. The shape of the centrality dependence of the second-harmonic signal is characteristic of anisotropic flow and quite different from possible non-flow sources.

Most commonly discussed non-flow sources of azimuthal correlations are: 1) Momentum conservation, which can be important for directed flow when each subevent is not symmetric about mid-rapidity, does not affect elliptic flow measurements. 2) Coulomb and Bose-Einstein correlations [23], which are eliminated by the construction of the subevents in Fig 2. 3) Resonance decay [24], whose effect on the subevent correlation would be independent of centrality and thus very different from that shown for the second harmonic. 4) Jets, when calculated using Hijing [22] for the cuts used in the current analysis, do not contribute beyond our quoted systematic error. Also, if jets or resonances contribute to v_2 they would contribute to the directed flow measurements in comparable amount [25]. The first harmonic correlation, which is shown in Fig 2, and the higher harmonics, are about an order of magnitude weaker than the elliptic flow at mid-centrality. These small correlation values set an upper limit for the contribution of all non-flow effects to the elliptic flow.

The correlation between two subevents can be used directly [2,3] to calculate the *average* elliptic flow for the particles used to determine the event planes. However, the method which allows for the calculation of elliptic flow as a function of p_t and rapidity and also for particles beyond the regions used for the event plane determination, involves correlation of the azimuthal angle, ϕ, of each particle with an event plane angle, Ψ, and then averaging over all events. In this paper we have used three particle correlation methods: 1) Correlating the particles from one hemisphere with the event plane of the subevent in the other hemisphere. 2) Correlating all the particles with the event plane of all the *other* particles. 3) Correlating particles of one charge sign with the event plane of the opposite charge sign.

Although the STAR detector has good azimuthal symmetry, small acceptance effects in the calculation of the event plane angle were removed by the methods of shifting or weighting [3]. This correction, by either method, is negligible for the second harmonic. The observed elliptic flow comes from the second harmonic Fourier coefficient of the particle azimuthal distribution with respect to the event plane which is simply $\langle\cos[2(\phi - \Psi_2)]\rangle$. The elliptic flow relative to the real reaction plane, Ψ_R, the plane defined by the impact parameter and the beam, can be evaluated by dividing the observed signal by the resolution, $\langle\cos[2(\Psi - \Psi_R)]\rangle$, of the event plane. The resolutions calculated from the correlation of subevent planes were somewhat different for the different subevent selections, but the resultant v_2 values were the same within statistical errors. The resolutions for the full events reach 0.7 for the centrality at the peak in Fig. 2, while in NA49 [12,13] at the SPS they only reached 0.4. A resolution of 0.7 is getting close to the ideal value of 1.0, which means that the correlation of other quantities, such as HBT measurements, with the event plane will be feasible. Since we do not measure the correlation with the first harmonic plane, we do not know the sign of v_2.

Our analysis procedures have been tested with simulated data [26] to which a known amount of flow has been added. The simulated data were filtered by a GEANT model of STAR and reconstructed in a similar way to that done for real data. For 2% and 10% elliptic flow added to the simulations, the flow extracted was (2.0 ± 0.1)% and (9.7 ± 0.2)%, respectively.

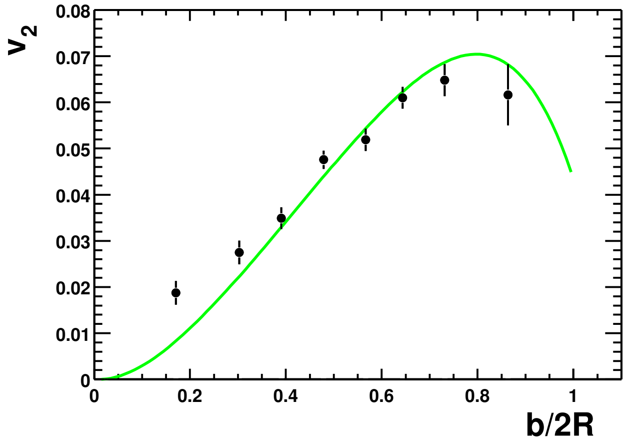

FIG. 3. Elliptic flow as a function of centrality defined from the fraction $\sigma_{top}/\sigma_{geo}$. The curve shows ϵ, the initial space eccentricity of the overlap region, multiplied by 0.16.

Fig. 3 shows v_2 as a function of centrality of the collision. The horizontal axis in this figure is chosen as $b/2R = \sqrt{\sigma_{top}/\sigma_{geo}}$, where the ratio $\sigma_{top}/\sigma_{geo}$ is calculated from Fig. 1 as the fraction of events corresponding to $n_{ch} > \langle n_{ch} \rangle_{bin}$. Note that in this scale, the most central events are on the left, opposite to the n_{ch} scale. The uncertainty of 10% mentioned for Fig. 1 would propagate to an uncertainty of 5% for $b/2R$. Although this figure was made with the subevents chosen as in Fig. 2, the same results within errors were obtained with the other correlation methods. Restricting the primary vertex z position to reduce TPC edge effects also made no difference. From the results of the study of non-flow contributions by different subevent selections and the maximum magnitudes of the first and higher-order harmonics, we estimate a systematic error for v_2 of about 0.005, with somewhat smaller uncertainty for the mid-centralities where the resolution of the event plane is high. The systematic errors are not included in the figures.

In the hydrodynamic limit, elliptic flow is approximately proportional to the initial space anisotropy, ϵ. In comparing the flow results to the curve for ϵ, calculated in Ref. [27], no unusual structure [4,19] is evident. The curve for ϵ shown in Fig. 3 is scaled such that $v_2/\epsilon = 0.16$. Hydrodynamic calculations predict [6,8] v_2/ϵ from 0.19 to 0.25. The lower value from the data could be due to a lack of equilibration during the time when the elliptic flow is generated [5,6]. Compared to RQMD predictions [18], v_2 peaks at a higher $b/2R$ value, in qualitative agreement with hydrodynamic expectations [7].

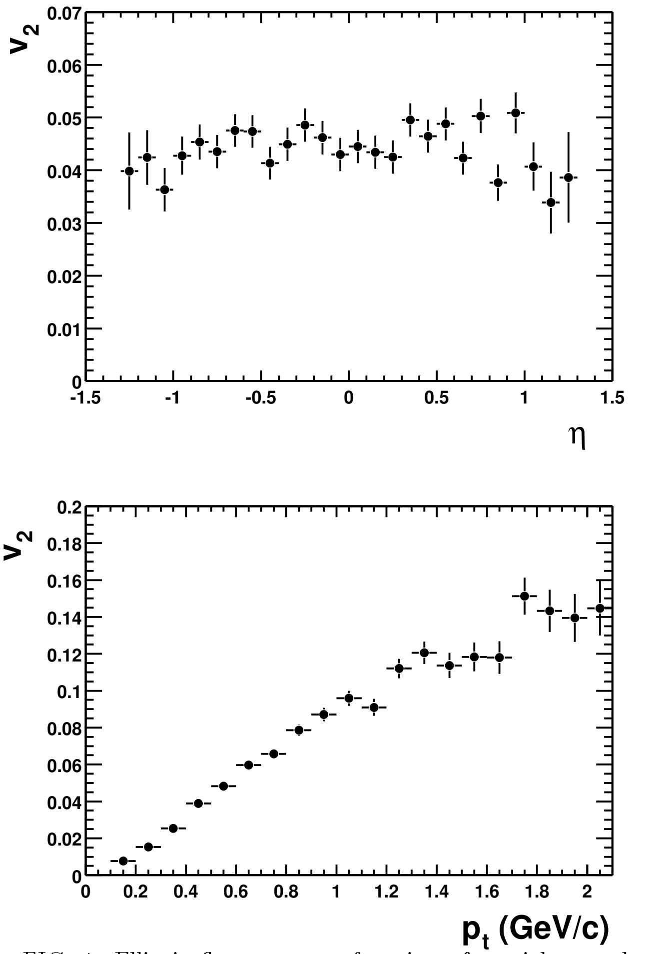

FIG. 4. Elliptic flow, v_2, as a function of particle pseudorapidity and transverse momentum for minimum bias events.

The differential anisotropic flow is a function of η and p_t. For the integrated results presented here, v should first be calculated as a function of η and p_t, and then averaged over either or both variables using the double differential cross sections as weights. Since we do not yet know the cross sections, we have averaged using the observed yields. Fig. 4 shows v_2 as a function of both η and p_t for a minimum bias trigger. For the η dependence, v_2 is averaged over p_t from 0.1 to 2.0 GeV/c. We have assumed that the efficiency (yield/cross section) is constant in the p_t range where the yield is large. This is borne out by studies of the effects of different track quality cuts on the observed p_t spectra. For the p_t dependence the data are not very sensitive to the assumption of constant efficiency as a function of η because they appear to be independent of η in the range used, $|\eta| < 1.3$. Mathematically the v_2 value at $p_t = 0$, as well as its first derivative, must be zero, but it is interesting that v_2 appears to rise almost linearly with p_t starting from relatively low values of p_t. This is consistent with a stronger "in-plane" hydrodynamic expansion of the system than the average radial expansion. Note that the results shown in Fig. 3 were obtained by taking the average over both η and p_t, weighted by the yield. Although Fig. 4 is for approximately minimum bias data [28] the general shapes are the same for data selected on centrality, except that the mean values on the η graphs and the slopes of the p_t curves depend on centrality. Fig. 4 was made using pseudorapidity subevents, although the same results within errors were obtained using the other methods.

We conclude that elliptic flow at RHIC rises up to about 6% for the most peripheral collisions, a value which is more than 50% larger than at the SPS [13], indicating stronger equilibration. Elliptic flow appears to be independent of pseudorapidity in the region $|\eta| \lesssim 1.3$. Its p_t dependence is almost linear in the region $0.1 < p_t < 2$ GeV/c. Comparing to estimates [18] based on transport cascade models, we find that elliptic flow is underpredicted by RQMD by a factor of more than 2. Hydrodynamic calculations [6,8] for RHIC energies overpredict elliptic flow by about 20-50%. The shape of the centrality dependence of the elliptic flow is similar to hydrodynamic calculations, consistent with significant thermalization. Yet, the lower values for elliptic flow indicate that early-time equilibration is still somewhat incomplete.

Acknowledgments: We wish to thank the RHIC Operations Group at Brookhaven National Laboratory for their tremendous support and for providing collisions for the experiment. This work was supported by the Division of Nuclear Physics and the Division of High Energy Physics of the Office of Science of the U.S.Department of Energy, the United States National Science Foundation, the Bundesministerium für Bildung und Forschung of Germany, the Institut National de la Physique Nucleaire et de la Physique des Particules of France, the United Kingdom Engineering and Physical Sciences Research Council, and the Russian Ministry of Science and Technology.

*Deceased

---

[1] For reviews and recent developments see *Quark Matter '99*, Nucl. Phys. **A661** (1999).
[2] S. Voloshin and Y. Zhang, Z. Phys. C **70**, 665 (1996).
[3] A.M. Poskanzer and S.A. Voloshin, Phys. Rev. C **58**, 1671 (1998).
[4] H. Sorge, Phys. Rev. Lett. **82**, 2048 (1999).
[5] S.A. Voloshin and A.M. Poskanzer, Phys. Lett. **B474**, 27 (2000).
[6] P. Kolb, J. Sollfrank, U. Heinz, preprint hep-ph/0006129.
[7] J.-Y. Ollitrault, Phys. Rev. D **46**, 229 (1992).
[8] P. Kolb, J. Sollfrank, U. Heinz, Phys. Lett. **B459**, 667 (1999).
[9] D. Teaney and E.V. Shuryak, Phys. Rev. Lett. **83**, 4951 (1999).
[10] E877 Collaboration, J. Barrette *et al.*, Phys. Rev. C **55**, 1420 (1997).
[11] E895 Collaboration, C. Pinkenburg *et al.* Phys. Rev. Lett. **83**, 1295 (1999).
[12] NA49 Collaboration, H. Appelshäuser *et al.*, Phys. Rev. Lett. **80**, 4136 (1998).
[13] A.M. Poskanzer and S.A. Voloshin for the NA49 Collaboration, Nucl. Phys. **A661**, 341c (1999).
[14] WA98 Collaboration, M.M. Aggarwal et al., Phys. Lett. B403 (1997) 390; M.M. Aggarwal *et al.*, Nucl. Phys. **A638**, 459 (1998).
[15] J.-Y. Ollitrault, Nucl. Phys. **A638**, 195c (1998).
[16] M. Bleicher and H. Stocker, preprint hep-ph/0006147.
[17] H. Sorge, Phys. Rev. **C 52**, 3291 (1995).
[18] R.J.M. Snellings, A.M. Poskanzer, and S.A. Voloshin, STAR Note SN0388 (1999), preprint nucl-ex/9904003.
[19] H. Heiselberg and A.-M. Levy, Phys. Rev. C **59**, 2716 (1999).
[20] STAR Collaboration, K.H. Ackermann *et al.*, Nucl. Phys. **A661**, 681c (1999).
[21] C. Adler *et al.*, preprint nucl-ex/0008005.
[22] M. Gyulassy and X.N. Wang, Comp. Phys. Comm. **83**, 307 (1994); Phys. Rev. **D44**, 3501 (1991).
[23] P.M. Dinh, N. Borghini, and J.-Y. Ollitrault, Phys. Lett. **B477**, 51 (2000).
[24] N. Borghini, P.M. Dinh, and J.-Y. Ollitrault, Phys. Rev. **C62**, 34902 (2000).
[25] Jet *quenching* could depend on the orientation of the jet with respect to the reaction plane. This would be a real flow correlation. Hijing predicts [18] the contribution of jet quenching to v_2 to be small at mid-rapidity for particles with $p_t < 2$ GeV/c.
[26] R.L. Ray and R.S. Longacre, STAR Note SN0419 (1999), preprint nucl-ex/0008009.
[27] P. Jacobs and G. Cooper, STAR Note SN0402 (1999), preprint nucl-ex/0008015. The $\varepsilon = \langle y^2 - x^2 \rangle / \langle y^2 + x^2 \rangle$ values used were for a Wounded Nucleon model with a Woods-Saxon potential.
[28] We say approximately because the quality cuts discriminate somewhat against the more central collisions. At each of the eight centralities, v_2 was calculated and the values were combined by weighting with the inverse of the square of the errors, which is proportional to the number of particles in that bin. This should be the same as a theoretical calculation of $\langle \cos(2\phi) \rangle$ of all particles in all events.